Supplementary Material (ESI) for Chemical Communications

Supporting Information

Controlled mineralization by extracellular matrix: monodisperse, colloidal stable calcium phosphate-hyaluronan hybrid nanospheres

Zhenhua Chen,[a] Huihui Zhou,[b] Xiaoliang Wang,[a] Lin Sang,[a] Caihong Wang,[a] Jianfeng Ma[a] and Xudong Li,*[a]

[a] National Engineering Research Center for Biomaterials, Sichuan University, Chengdu 610064, PR China

[b] College of Materials Science and Engineering, Sichuan University, Chengdu 610064, PR China

Summary: 9 Pages, 2 Tables, 6 Figures

1. **Table S1.** Sample preparation and designation of the synthetic calcium phosphate nanoparticles in the absence and presence of hyaluronan

Sample	Hya /g	$CaCl_2$ /g	$NaH_2PO_4 \cdot 2H_2O$ /g	H_2O /mL	Initial pH	Morphology	Size /nm
HC-0	0	1.11	0.936	100	4.68	sheet	aggregate
HC-1	0.040	1.11	0.936	100	4.69	conjugate	aggregate
HC-2	0.10	1.11	0.936	100	4.72	conjugate	aggregate
HC-3	1.0	1.11	0.936	100	5.06	sphere	40

2. **Table S2** Zeta potentials of the synthetic calcium phosphate nanoparticles measured at pH=7.0, T=290.2K

sample	HC-0	HC-1	HC-2	HC-3
reaction condition	without Hya	with Hya (0.04g)	with Hya (0.1g)	with Hya (1.0g)
zeta potential/mV	0.40	-1.6	-11.7	-17.1

3. **Fig. S1** SEM image of the synthetic calcium phosphate nanoparticles obtained in the absence of hyaluronan.

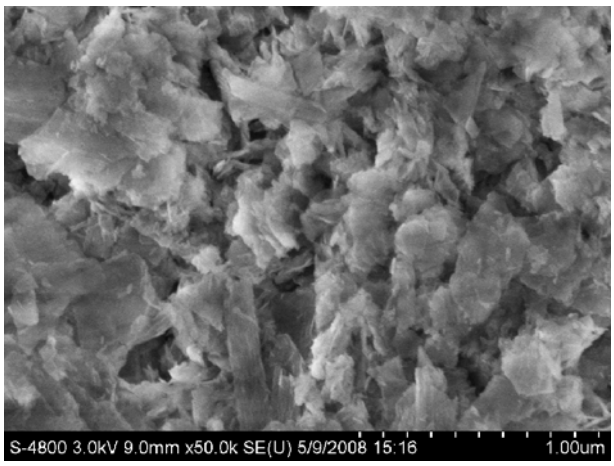

4. **Fig. S2** SEM image of the synthetic calcium phosphate nanoparticles (HC-3) after storage in water for 45 days.

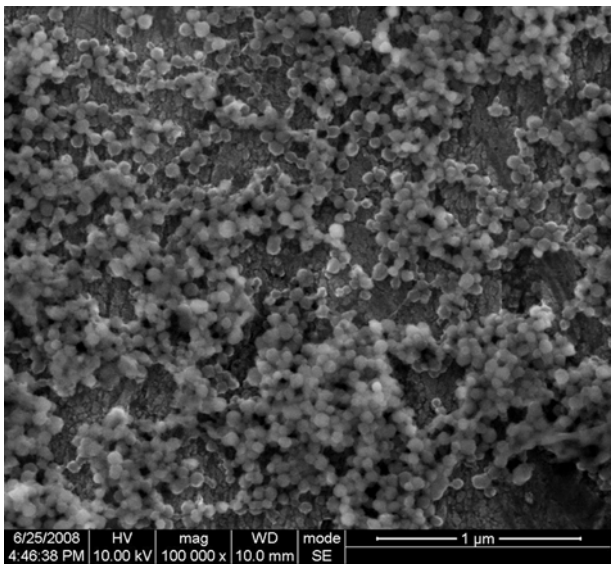

5. **Fig. S3** TEM image of calcium phosphate nanoparticles (HC-3) after storage in water for 180 days.

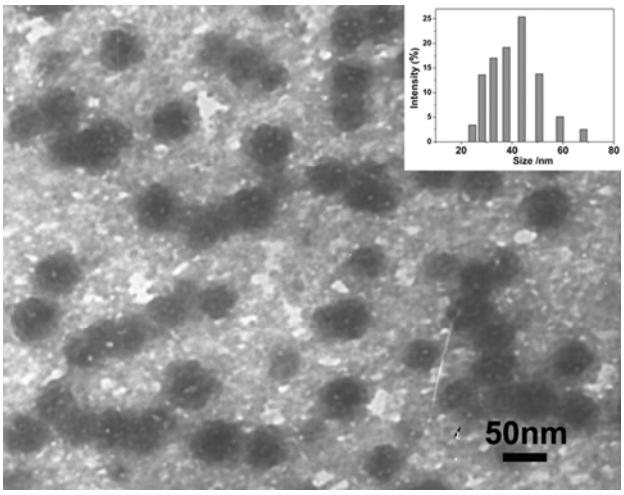

6. **Fig. S4.** FTIR spectra of the synthetic calcium phosphate nanoparticles in the absence and presence of hyaluronan.

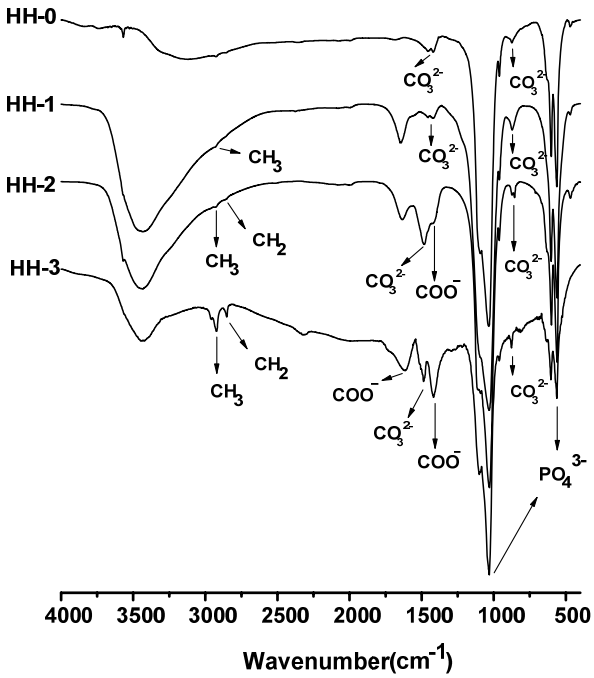

7. **Fig. S5** Viscosity of hyaluronan at various concentrations in the absence and presence of 0.1M Ca^{2+}

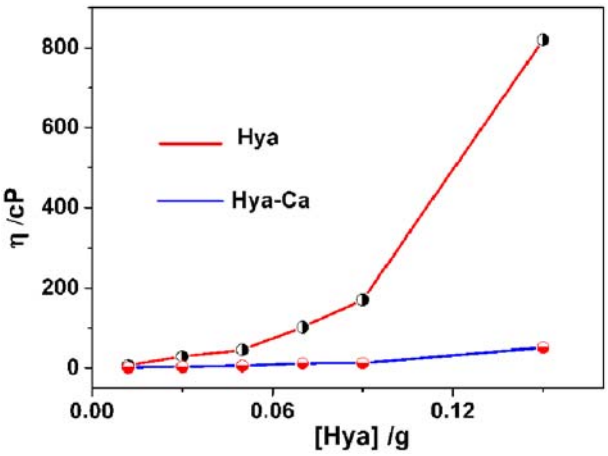

8. **Fig. S6** Conductivity of hyaluronan at various concentrations in the absence (Λ_{Hya}) and presence of 0.1M Ca^{2+} ($\Lambda_{Hya\text{-}Ca}$). $\Lambda_{Hya\text{-}Ca} - \Lambda_{Hya}$ indicates that the increase of added hyaluronan significantly decreased the conductivity of Ca^{2+} (0.1M)

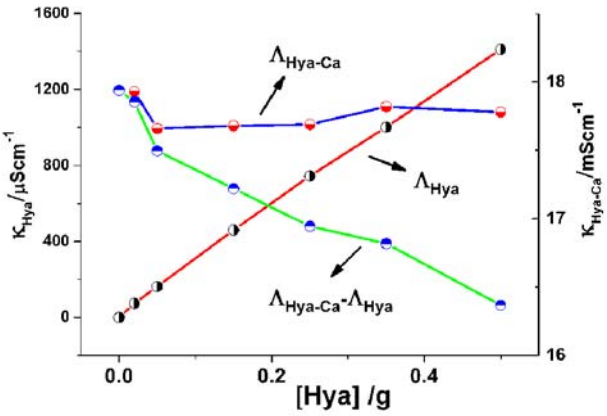

9. **Viscosity experiment of hyaluronan at various concentrations in the absence and presence of 0.1 M Ca^{2+}**

To validate the complexation between hyaluronan (Hya) and calcium ions exists, the viscosity experiment of hyaluronan at various concentrations in the absence and presence of 0.1M $CaCl_2$ was performed. The added amount of Hya varied from 0.012 to 0.15g. Every specimen for viscosity experiment has a volume of 30 mL. Viscosities for the Hya and Hya-Ca systems were measured with a suspended level Ubbelohade viscometer that had a flow time of about 200 s for water at 298.15 K. Flow time measurements were performed by a Schott AVS 310 photoelectric time unit (Schott, Germany) with a resolution of 0.01 s. At least three time recordings reproducible to 0.02 s were obtained, and the average value was used in the calculations. The viscosity of the solution, η, is given by the following equation:

$$\eta / \rho = Bt - C / t \qquad (1)$$

Where ρ is the solution density determined by an Anton Paar DMA 60/602 vibrating-tube digital densimeter, t is the flow time, and B and C are the viscometer constants obtained by the measurements on water at 298.15 and 308.15 K. The densimeter and viscometer were thermostated using Schott thermostat units, which have a thermal stability of ±0.01 K. The viscosities for the Hya and Hya-Ca systems are presented in Fig. S5. The presence of Ca^{2+} significantly slowed down the increase of the Hya viscosity with a higher concentration.

10. **Conductivity experiment of hyaluronan at various concentrations in the absence and presence of 0.1 M Ca^{2+}**

To further confirm the complexing interactions between Hya and Ca^{2+}, the

conductivity experiment of hyaluronan at various concentrations in the absence and presence of 0.1 M $CaCl_2$ was performed. The added amount of Hya varied from 0.02 to 0.5 g. Every specimen for conductivity experiment has a volume of 50 mL. Conductivities for the Hya and Hya-Ca systems were measured by a Mettler Toledo conductometer (Sevenmulti, Mettler Toledo, Switzerland) at 298.15 K. The conductance cell was equipped with a water circulating jacket, and the temperature was controlled within ± 0.03 K with a DC-2006 low temperature thermostat (shanghai, Hengping Instrument Factory). The cell was calibrated with aqueous KCl solutions at different concentrations, and a cell constant of 0.784618 cm^{-1} was determined. The conductivities for the Hya and Hya-Ca systems were shown in Fig. S6. $\Lambda_{Hya\text{-}Ca}$-Λ_{Hya} (Fig. S6) indicates that a higher amount of added hyaluronan significantly decreased the conductivity of Ca^{2+} (0.1M), suggesting that Hya has a strong capability to constrain the migration of free Ca^{2+} ions.

11. **Preparation of Hya-CaP hybrid nanoparticles**

The mineralization of CaP nanoparticles was carried out using ammonia diffusion method. In all experiments, initial Ca^{2+}, $H_2PO_4^-$ concentration was fixed at 0.1 M and 0.06 M, respectively. Varying mass fraction of Hya from 0, 0.04, 0.1, to 1.0 g was introduced to constitute four CaP synthesis groups for investigating the Hya modulation of CaP mineralization. Thus, we designated as HC-0, HC-1, HC-2, and HC-3, respectively (see Table S1). In a typical procedure, a mixture of sodium hyaluronate (1.0 g, 8.47×10^{-4} mM, Mw=1180 kDa), anhydrous $CaCl_2$ (1.11 g, 0.1 M), dehydrate NaH_2PO_4 (0.936 g, 0.06 M) and deionized water (5.53 mol, 100 mL, MilliQ,

18.3 MΩ·cm) was oscillated using a vortex (IKA, Genius 3) to form homogeneous solution (pH=5.06). Then, the solution was poured into a flask and the flask was covered with aluminum foil and punctured a few holes with a needle. Another flask was filled with 100m L concentrated ammonia (28% w/w) and also covered with aluminum foil punctured with several holes. Subsequently, both flasks were placed in a closed desiccator at room temperature for two weeks. The vessel was left still in a fume cupboard prior to harvesting the crystals. The white sol containing CaP precipitate was first filtered using microporous membrane (0.45 μm, Millipore) to remove any exogenous dust or impurities. Then, the CaP nanoparticles were separated from the filtered sol solution by centrifugation (5×10^4 g min^{-1}, for 30 min) and rinsed with deionized water thoroughly and air-dried for further analysis.

12. **Colloidal stability measurement of HC-3 nanoparticles**

To study the colloidal stability of synthetic HC-3 nanoparticles in aqueous solution, we dispersed the obtained HC-3 nanoparticles into deionized water to form a suspension and left it still for 45 days and 180 days at ambient condition. Then, we examined the morphology and size of the nanoprticles after having kept still for 45 days and 180 days by scanning electron microscopy (SEM S4800, Hitachi, Japan), transmission electron microscopy (TEM, JEM-100CX, Japan) and dynamic light scattering (DLS, NanoS ZEN 3600, Malvern, UK). After the suspension was kept still for 45 days, a drop of the suspension (5μL) was settled on the SEM substrate and vaporized the excessive water. Then, morphology of the sample was directly examined without gold coating. SEM image shown in Fig.S2 reveals that after having

been suspended and storaged in water for 45days, the HC-3 nanoparticles still maintain its original monodisperse spherical shape (Fig. 1B). The average size of the nanospheres in Fig. S2 is 40nm (the same size as the nanospheres shown in Fig.1B). After the HC-3 nanoparticles' suspension has kept still for 180 days, TEM and DLS were used to confirm the colloidal stability of the synthetic nanospheres. TEM and DLS results shown in Fig. S3 indicate that the HC-3 nanospheres after storage for 180 days still maintain their spherical shape with a size distribution ranged from 20 to 60 nm in diameter.

13. **Physical and chemical characterization of the nanoparticles obtained from HC-0 to HC-3 by FTIR and Zeta potentials**

To identify the composition of the synthetic nanoparticles, FTIR spectra of the products obtained from HC-0 to HC-3 and pure Hya were performed by using a Perkin-Elmer spectrum one B system with a resolution of 4.00 cm^{-1}. Standard KBr disks method was adopted. FTIR spectra shown in Fig. S4 suggest that all the nanoparticles obtained from HC-0 to HC-3 posses the characteristic adsorptions of hydroxyapatite, and that more Hya has been incorporated into the nanoparticles with increasing Hya dosage at the initial of the mineralization. To further confirm that more Hya was incorporated into the nanoparticles from HC-0 to HC-3, Zeta potentials of the corresponding samples were performed by using a Malvern NanoS ZEN 3600 instrument (calibrated using the protocol of "Zeta Transfer Standard"). All measurements were averaged 12 runs using deionized water at pH=7, 290.2K. The results listed in Table S2 indicate that the nanoparticles became more negatively charged with a higher amount of added Hya into the mineralisation system.